A Discontinuous Galerkin Solver for Full-Band Boltzmann-Poisson Models

Yingda Cheng
and Irene M. Gamba
Department of Mathematics and ICES
The University of Texas at Austin
Austin, TX 78712
Email: ycheng@math.utexas.edu
Email: gamba@math.utexas.edu

Armando Majorana
Dipartimento di Matematica e Informatica
Università di Catania
Catania, Italy
Email: majorana@dmi.unict.it

Chi-Wang Shu
Division of Applied Mathematics
Brown University
Providence, RI 02912
Email: shu@dam.brown.edu

***Abstract*—We present new preliminary results of a discontinuous Galerkin (DG) scheme applied to deterministic computations of the transients for the Boltzmann-Poisson (BP) system describing electron transport in semiconductor devices. Very recently in [1], [2], [3], results for one and two dimensional devices were obtained in the case of silicon semiconductor assuming the non-parabolic band approximation. Here, more general band structures are considered. Preliminary benchmark numerical tests on Kane and Brunetti et al. band models are reported.**

I. Introduction

In modern highly integrated devices, the charge carrier transport can be described by the semiclassical Boltzmann-Poisson (BP) system.

$$\frac{\partial f}{\partial \mathrm{t}} + \frac{1}{\hbar}\nabla_{\underline{\mathsf{k}}}\,\varepsilon \cdot \nabla_{\underline{\mathsf{x}}} f - \frac{q}{\hbar}\underline{\mathsf{E}} \cdot \nabla_{\underline{\mathsf{k}}} f = Q(f)\,, \tag{1}$$

$$\nabla_{\underline{\mathsf{x}}}\left[\epsilon_r(\underline{\mathsf{x}})\,\nabla_{\underline{\mathsf{x}}} V\right] = \frac{q}{\epsilon_0}\left[n(\mathrm{t},\underline{\mathsf{x}}) - N_D(\underline{\mathsf{x}})\right],\ \underline{\mathsf{E}} = -\nabla_{\underline{\mathsf{x}}} V\,. \tag{2}$$

Time-dependent solutions of the above system contain all the information on the transient of the carrier distribution.

In Eq. (1), f represents the electron probability density function in phase space $\underline{\mathsf{k}}$ at the physical location $\underline{\mathsf{x}}$ and time t. The electric field is denoted by $\underline{\mathsf{E}}$ and ε is the energy-band function. Physical constants $\hbar$ and q are the Planck constant divided by 2π and the positive electric charge, respectively. The collision operator $Q(f)$ describes electron-phonon interactions where the most important ones in Si are due to scattering with lattice vibrations of the crystal, which are modeled by acoustic and optical non-polar modes with a single frequency ω_p, i.e.

$$Q(f) = \int_{\Omega_{\underline{\mathsf{k}}}} \left[S(\underline{\mathsf{k}}', \underline{\mathsf{k}}) f(\mathrm{t}, \underline{\mathsf{x}}, \underline{\mathsf{k}}') - S(\underline{\mathsf{k}}, \underline{\mathsf{k}}') f(\mathrm{t}, \underline{\mathsf{x}}, \underline{\mathsf{k}})\right] d\underline{\mathsf{k}}' \tag{3}$$

where $S(\mathsf{k}, \mathsf{k}')$ is defined by

$$\begin{aligned} S(\underline{\mathsf{k}}, \underline{\mathsf{k}}') &= (n_q + 1)\, K\, \delta(\varepsilon(\underline{\mathsf{k}}') - \varepsilon(\underline{\mathsf{k}}) + \hbar\omega_p) \\ &+ n_q\, K\, \delta(\varepsilon(\underline{\mathsf{k}}') - \varepsilon(\underline{\mathsf{k}}) - \hbar\omega_p) + K_0\, \delta(\varepsilon(\underline{\mathsf{k}}') - \varepsilon(\underline{\mathsf{k}}))\,, \end{aligned}$$

and K, K_0 are constants. The phonon occupation factor is

$$\mathsf{n}_q = \left[\exp\left(\frac{\hbar\omega_p}{k_B T_L}\right) - 1\right]^{-1},$$

where k_B is the Boltzmann constant and $T_L = 300^\circ K$ is the constant lattice temperature. The symbol δ indicates the usual Dirac distribution. In Eq. (2), ϵ_0 is the dielectric constant in a vacuum, $\epsilon_r(\mathbf{x})$ labels the relative dielectric function depending on the material, $\rho(t, \mathbf{x})$ is the electron density, and $N_D(\mathbf{x})$ is the doping. Eq. (1) can be easily generalized to more valleys by replacing f with an array and including the intervalley scattering terms in the collisional operator.

After the pioneer work [4], in recent years, deterministic solvers to the BP system were proposed [1]-[3], [5], [6], [7], [8]. These methods provide accurate results which, in general, agree well with those obtained from Monte Carlo (DSMC) simulations, often at a fractional computational time. Moreover, they can resolve transient details for the electron probability density function f, which are difficult to compute with DSMC simulators.

In all of the aforementioned deterministic solvers, the energy-band function $\varepsilon(\underline{\mathsf{k}})$ is given analytically, either by the parabolic band approximation or by the Kane non-parabolic band model. The analytical band makes use of the explicit dependence of the carrier energy on the quasimomentum, which significantly simplifies all expressions as well as implementation of these techniques. However, the physical details of the band structure are partly or totally ignored, which hinders the application to transport of hot carriers in high-field phenomena with highly anisotropic band structure. Full band models, on the other hand, can guarantee accurate physical pictures of the energy-band function. They are widely used in DSMC simulators, but only recently the transport Boltzmann equation was considered [9], [10], where approximate solutions were found by means of spherical harmonics expansion of the distribution function f. Since only a few terms of the expansion are usually employed, high accuracy is not always achieved [11]. Our model and simulation [1]-[3] do not involve any asymptotics to approximate the BP system.

II. Numerical Algorithm

We propose a discontinuous Galerkin (DG) solver to full band BP models. It is a generalization of the scheme for the Kane non-parabolic band relations developed in [1]-[3]. The

DG scheme is a conservative scheme that has the advantage of flexibility for arbitrarily unstructured meshes and the full potential for arbitrary *hp*-adaptivity. In this paper, we adapt this solver to treat the full band case. The main advantage of this solver is that the direct evaluation of the Dirac delta function can be avoided. Hence, an accurate yet high-order simulation with comparable computational cost to the analytic band cases is possible.

A. Change of Variables

Unlike [3], the coordinate transform proposed in [12], which is based on the analytic band relation, can no longer be used. However, it is still desired to use the spherical coordinate systems compared to the cartesian coordinates in $\underline{\mathsf{k}}$ space because of the much higher resolution demands near the point $\underline{\mathsf{k}} = 0$ and the consideration that away from the origin large cells are sufficient for describing the tail of the distribution function accurately. We remark that the new coordinate does not require symmetry of the problem, so the anisotropic band case can be computed without additional difficulty.

We assume that the typical values for length, time and voltage are $\ell_* = 10^{-6}\, m$, $t_* = 10^{-12}\, s$ and $V_* = 1\,\text{Volt}$, respectively. The following dimensionless quantities and change of variables are introduced for general three-dimensional device.

$$t = \frac{\mathrm{t}}{t_*}\,, \quad (x,y,z) = \frac{\underline{\mathsf{x}}}{\ell_*}\,,$$

$$\underline{\mathsf{k}} = \frac{\sqrt{2m^* k_B T_L}}{\hbar}\sqrt{r}\left(\mu, \sqrt{1-\mu^2}\cos\varphi, \sqrt{1-\mu^2}\sin\varphi\right)$$

with $r \geq 0\,, \mu \in [-1,1]\,, \varphi \in [-\pi,\pi]\,,$

$$\mathcal{E}(r,\mu,\varphi) = \frac{1}{k_B T_L}\varepsilon(\underline{\mathsf{k}})$$

$$\Psi(t,x,y,z) = \frac{V(t_*\,t, \ell_*\,x, \ell_*\,y, \ell_*\,z)}{V_*}$$

$$\underline{\mathsf{E}} = -c_v \nabla_{\underline{\mathsf{x}}} V \text{ with } c_v = \frac{V_*}{\ell_* E_*} \text{ and } E_* = 0.1\, V_*\, \ell_*^{-1}\,.$$

The spherical coordinates map the $\underline{\mathsf{k}}$-domain $\Omega_{\underline{\mathsf{k}}}$ onto the set Ω of the (r,μ,φ) space. Now, the new unknown function Φ is obtained by the f multiplied by the Jacobian of transformation

$$\Phi(t,x,y,z,r,\mu,\varphi) = \frac{1}{2}\sqrt{r}\, f(t,x,y,z,r,\mu,\varphi)\,,$$

and it satisfies the following equation

$$\frac{\partial \Phi}{\partial t} + \frac{\partial}{\partial x}(a_1\,\Phi) + \frac{\partial}{\partial y}(a_2\,\Phi) + \frac{\partial}{\partial z}(a_3\,\Phi) + \frac{\partial}{\partial r}(a_4\,\Phi) + \frac{\partial}{\partial \mu}(a_5\,\Phi) + \frac{\partial}{\partial \varphi}(a_6\,\Phi) = C(\Phi), \tag{4}$$

where

$$a_1(\cdot) = c_D\left(2\sqrt{r}\,\mu\,\frac{\partial \mathcal{E}}{\partial r} + \frac{1-\mu^2}{\sqrt{r}}\frac{\partial \mathcal{E}}{\partial \mu}\right),$$

$$a_2(\cdot) = c_D\left(2\sqrt{r}\sqrt{1-\mu^2}\cos\varphi\,\frac{\partial \mathcal{E}}{\partial r} - \frac{\mu\sqrt{1-\mu^2}\cos\varphi}{\sqrt{r}}\frac{\partial \mathcal{E}}{\partial \mu} - \frac{\sin\varphi}{\sqrt{r}\sqrt{1-\mu^2}}\frac{\partial \mathcal{E}}{\partial \varphi}\right),$$

$$a_3(\cdot) = c_D\left(2\sqrt{r}\sqrt{1-\mu^2}\sin\varphi\,\frac{\partial \mathcal{E}}{\partial r} - \frac{\mu\sqrt{1-\mu^2}\sin\varphi}{\sqrt{r}}\frac{\partial \mathcal{E}}{\partial \mu} + \frac{\cos\varphi}{\sqrt{r}\sqrt{1-\mu^2}}\frac{\partial \mathcal{E}}{\partial \varphi}\right),$$

$$a_4(\cdot) = -2\,c_E\sqrt{r}\left[\mu\,E_x(t,x,y,z) + \sqrt{1-\mu^2} \times (\cos\varphi\,E_y(t,x,y,z) + \sin\varphi\,E_z(t,x,y,z))\right],$$

$$a_5(\cdot) = -c_E\left[\frac{1-\mu^2}{\sqrt{r}}\,E_x(t,x,y,z) - \frac{\mu\sqrt{1-\mu^2}}{\sqrt{r}} \times (\cos\varphi\,E_y(t,x,y,z) + \sin\varphi\,E_z(t,x,y,z))\right],$$

$$a_6(\cdot) = -c_E\,\frac{1}{\sqrt{r}\sqrt{1-\mu^2}}\left[-\sin\varphi\,E_y(t,x,y,z) + \cos\varphi\,E_z(t,x,y,z)\right],$$

and

$$C(\Phi)(t,x,y,z,r,\mu,\varphi) = \frac{1}{2}\sqrt{r}\int_\Omega \left[\mathcal{S}(r',\mu',\varphi',r,\mu,\varphi)\,\Phi(t,x,y,z,r',\mu',\varphi')\,dr'\,d\mu' d\varphi'\right] - \Phi(t,x,y,z,r,\mu,\varphi) \times \int_\Omega \mathcal{S}(r,\mu,\varphi,r',\mu',\varphi')\,\frac{1}{2}\sqrt{r'}\,dr'\,d\mu' d\varphi'\,, \tag{5}$$

where

$$\mathcal{S}(r,\mu,\varphi,r',\mu',\varphi') = c_+\,\delta(\mathcal{E}(r',\mu',\varphi') - \mathcal{E}(r,\mu,\varphi) + \alpha_p) + c_-\,\delta(\mathcal{E}(r',\mu',\varphi') - \mathcal{E}(r,\mu,\varphi) - \alpha_p) + c_0\,\delta(\mathcal{E}(r',\mu',\varphi') - \mathcal{E}(r,\mu,\varphi)),$$

is the scattering kernel. The constants are listed below

$$c_D = \frac{t_*}{\ell_*}\sqrt{\frac{k_B T_L}{2\,m^*}}\,, \quad c_E = \frac{t_* q E_*}{\sqrt{2m^* k_B T_L}}\,, \quad \alpha_p = \frac{\hbar\omega_p}{k_B T_L},$$

$$(c_+, c_-, c_0) = \frac{2m^*\,t_*}{\hbar^3}\sqrt{2\,m^*\,k_B T_L}\,[(n_q+1)K, n_q K, K_0]\,.$$

The dimensionless Poisson equation is

$$\frac{\partial}{\partial x}\left(\epsilon_r\frac{\partial \Psi}{\partial x}\right) + \frac{\partial}{\partial y}\left(\epsilon_r\frac{\partial \Psi}{\partial y}\right) + \frac{\partial}{\partial z}\left(\epsilon_r\frac{\partial \Psi}{\partial z}\right) = c_p\left[\rho(t,x,y,z,t) - \mathcal{N}_D(x,y,z)\right], \tag{6}$$

where

$$\mathcal{N}_D(x,y,z) = \left(\frac{\sqrt{2\,m^* k_B T_L}}{\hbar}\right)^{-3} N_D(\ell_* x, \ell_* y, \ell_* z),$$

$$\rho(t,x,y,z) = \int_\Omega \Phi(t,x,y,z,r',\mu',\varphi')\,dr'\,d\mu' d\varphi'\,,$$

$$c_p = \left(\frac{\sqrt{2\,m^* k_B T_L}}{\hbar}\right)^3 \frac{\ell_*^2 q}{\epsilon_0\, V_*}\,.$$

B. DG Formulation

The DG scheme for Eq. (4) is similar to its counterpart in [3] except for terms involving the energy band. When solving Eq. (4), the solution within each computational element of the (x,y,z,r,μ,φ) domain is assumed to be a polynomial (linear in our computation) in the (x,y,z) and (r,μ,φ) variables having unknown time-dependent coefficients. The resulting

equations are ordinary differential equations for those coefficients which can be solved by a suitable Runge-Kutta time discretization. Eq. (6) is solved by the local DG (LDG) method proposed in [13]. We refer to [3] for more details about the treatment of different boundary conditions for various devices.

The drift terms a_1, a_2, a_3 and the collision term (5) involve the numerical band data. A smooth interpolant of $\mathcal{E}$ on each computational element indexed by α in (r, μ, φ) space is generated as follows,

$$\mathcal{E}(r,\mu,\varphi) = \mathcal{E}(r_\alpha,\mu_\alpha,\varphi_\alpha) + A_{\alpha,r}\,(r-r_\alpha) + A_{\alpha,\mu}\,(\mu-\mu_\alpha) + A_{\alpha,\varphi}\,(\varphi-\varphi_\alpha)\,,$$

where the coefficients $\mathcal{E}(r_\alpha,\mu_\alpha,\varphi_\alpha)$, $A_{\alpha,r}$, $A_{\alpha,\mu}$, $A_{\alpha,\varphi}$ are pre-computed based on the numerical band input. The point $(r_\alpha,\mu_\alpha,\varphi_\alpha)$ is the center of the cell α. A similar expression is used to approximate the the group velocity in each cell. This simple description enables us to compute the collision and the drift terms effectively and is accurate enough for our application.

III. Numerical Results

We present some preliminary results based on the Kane band model and Brunetti et al. band model [14]. The Kane dispersion relation is given by,

$$\varepsilon(1+\alpha_K\varepsilon) = \frac{\hbar^2 k^2}{2m^*}\,, \tag{7}$$

where α_K is the non-parabolicity factor and m^* the effective electron mass. The Brunetti et al. model used a non parabolic approximation for energy less then $1.75eV$ and a simple parabolic function for high energy. Now, the approach used in [1]-[3], [5]-[7], [12], where a transformation of variables allows a simple treatment of the kernel of the collision operator, is not available, since the electron energy function is not a monotone function of $\|\underline{k}\|^2$. Figure 1 shows a comparison of the two band models. We benchmark the scheme on the test case of Si $n^+ - n - n^+$ diode with channel length of 400nm.

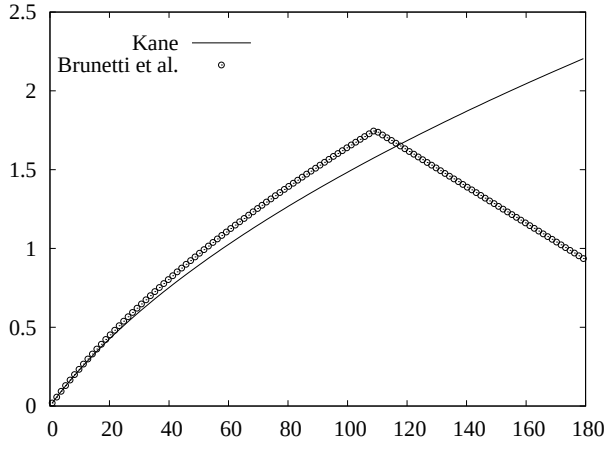

Fig. 1. Comparison of the Kane and Brunetti band models. r versus electron energy (in eV).

Details about the configuration of the device can be found in [6]. The results are obtained by using the analytic formula (7) and the discrete band data respectively. The discrete band data is obtained as follows. The Kane band model can be rewritten in the new set of coordinates (r,μ,φ) as

$$\mathcal{E}(r) = \frac{2\,r}{1+\sqrt{1+4\,\hat{\alpha}_K\,r}}\,, \quad \hat{\alpha}_K = \alpha_K\,k_B T_L\,.$$

After a first-order Taylor expansion, the discrete version of the model is

$$\mathcal{E}(r,\mu,\varphi) = \mathcal{E}(r_\alpha) + A_{\alpha,r}\,(r-r_\alpha),$$

where

$$\mathcal{E}(r_\alpha) = \frac{2\,r_\alpha}{1+\sqrt{1+4\,\hat{\alpha}_K\,r_\alpha}}, \quad A_{\alpha,r} = \frac{1}{\sqrt{1+4\,\hat{\alpha}_K r_\alpha}}\,.$$

We then use the algorithm described in Section II to compare the results computed in [3] for the analytic band. In Figure 2, we plot the velocity and energy for the diodes at $t = 0.5$ps, when the device is still in transient state. Results for density of charge coincide in all the cases. They show the good agreement between the analytical and numerical Kane electron energy model for higher order moments. In particular, the results for numerical and analytical Kane band model benchmark our solver, justifying our approach of treating the full band models.

The discrete Brunetti et al. band can be computed similarly by a first-order Taylor expansion. In Figure 3, we compare the results at $t = 4$ps, when the device has reached steady states. The discrepancies in Figures 2 and 3 for mean velocities and kinetic energies with respect to the Kane and Brunetti et al. model in the channel region are expected, since the band energy above $1.75eV$ differ significantly as can be seen in Figure 1.

IV. Conclusion

We propose a DG algorithm for full-band BP models. Benchmark test cases based on the Kane and Brunetti band models are given. Future work includes implementing the scheme for anisotropic band and numerical band data.

Acknowledgment

The second author is supported by NSF grants DMS-0807712 and FRG-0757450. The third author is supported by the EU Marie Curie RTN project COMSON grant n. MRTN-CT-2005-019417. The fourth author is supported by NSF grant DMS-0809086 and DOE grant DE-FG02-08ER25863. Support from the Institute of Computational Engineering and Sciences and the University of Texas at Austin is also gratefully acknowledged.

References

[1] Y. Cheng, I. M. Gamba, A. Majorana, and C.-W. Shu, "Discontinuous Galerkin solver for the semiconductor Boltzmann equation," *SISPAD 07, June 14-17*, pp. 257–260, 2007.

[2] ——, "Discontinuous Galerkin solver for Boltzmann-Poisson transients," *J. Comput. Electron.*, vol. 7, pp. 119–123, 2008.

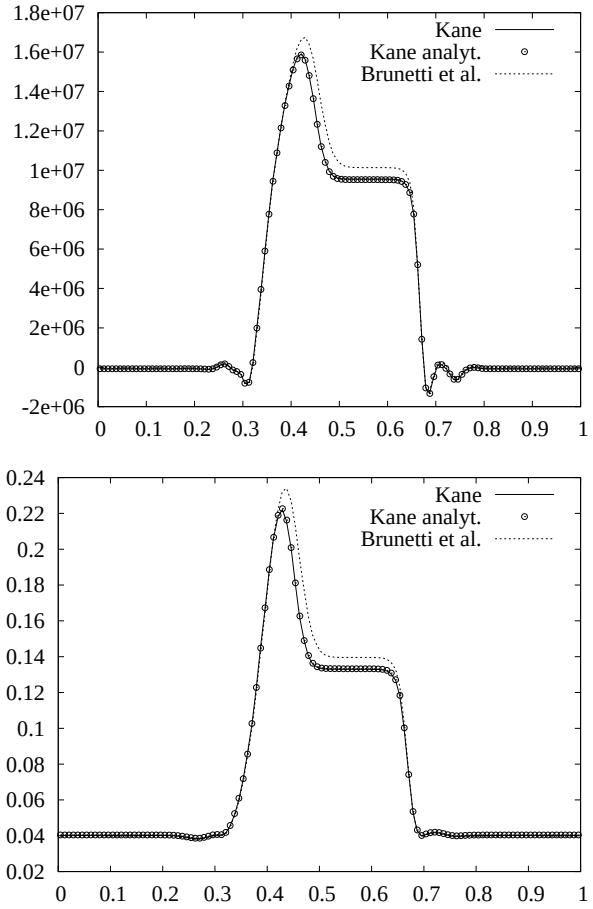

Fig. 2. Velocity (top) in cm/sec and kinetic energy (bottom) in eV of the 400nm channel diode at $t = 0.5$ps.

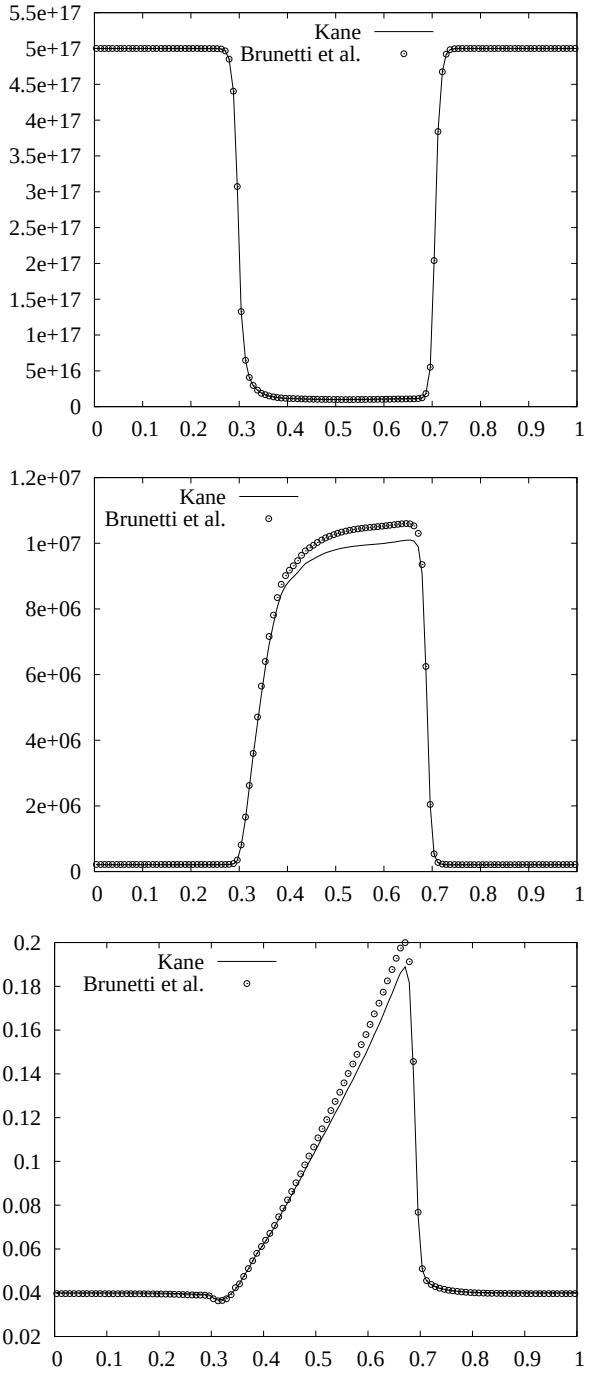

Fig. 3. Comparison of the Kane and Brunetti et al. models for 400nm channel diode at $t = 4$.ps. Density (top) in cm^{-3}, velocity (middle) in cm/sec and kinetic energy (bottom) in eV.

[3] ——, "A Discontinuous Galerkin solver for Boltzmann-Poisson systems for semiconductor devices," preprint submitted to Comput. Methods Appl. Mech. Eng., *in revision*.

[4] E. Fatemi and F. Odeh, "Upwind finite difference solution of Boltzmann equation applied to electron transport in semiconductor devices," *J. Comput. Phys.*, vol. 108, pp. 209–217, 1993.

[5] J. A. Carrillo, I. M. Gamba, A. Majorana, and C.-W. Shu, "A WENO-solver for 1D non-stationary Boltzmann-Poisson system for semiconductor devices," *J. Comput. Electron.*, vol. 1, pp. 365–375, 2002.

[6] ——, "A WENO-solver for the transients of Boltzmann-Poisson system for semiconductor devices. performance and comparisons with Monte Carlo methods," *J. Comput. Phys.*, vol. 184, pp. 498–525, 2003.

[7] ——, "2D semiconductor device simulations by WENO-Boltzmann schemes: efficiency, boundary conditions and comparison to Monte Carlo methods," *J. Comput. Phys.*, vol. 214, pp. 55–80, 2006.

[8] M. Galler and A. Majorana, "Deterministic and stochastic simulation of electron transport in semiconductors," *6th MAFPD (Kyoto) special issue Vol. 2*, pp. 349–365, 2007.

[9] M. C. Vecchi, D. Ventura, A. Gnudi, and G.Baccarani, "Incorporating full band-structure effects in spherical harmonics expansion of the Boltzmann transport equation," *Proceedings of NUPAD V Conference*, vol. 8, pp. 55–58, 1994.

[10] S. Smirnov and C. Jungemann, "A full band deterministic model for semiclassical carrier transport in semiconductors," *J. Appl. Phys.*, vol. 99, p. 063707, 1988.

[11] A. Majorana, "A comparison between bulk solutions to the Boltzmann equation and the spherical harmonic model for silicon devices," *Progress in Industrial Mathematics at ECMI 2000 - Mathematics in Industry*, vol. 1, pp. 169–173, 2002.

[12] A. Majorana and R. Pidatella, "A finite difference scheme solving the Boltzmann Poisson system for semiconductor devices," *J. Comput. Phys.*, vol. 174, pp. 649–668, 2001.

[13] B. Cockburn and C.-W. Shu, "The local discontinuous Galerkin method for time-dependent convection-diffusion systems," *SIAM J. Numer. Anal.*, vol. 35, pp. 2440–2463, 1998.

[14] R. Brunetti, C. Jacoboni, F. Venturi, E. Sangiorgib, and B. Riccò, "A many-band silicon model for hot-electron transport at high energies," *Solid State Electron.*, vol. 32, p. 1663, 1989.